

A Study on Transmission Characteristics and Specific Absorption Rate Using Impedance-Matched Electrodes for Various Human Body Communication

Yuta Machida, Takahiko Yamamoto, Kohji Koshiji, *Member, IEEE*

Abstract—Human body communication (HBC) is a new communication technology that has presented potential applications in health care and elderly support systems in recent years. In this study, which is focused on a wearable transmitter and receiver for HBC in a body area network (BAN), we performed electromagnetic field analysis and simulation using the finite difference time domain (FDTD) method with various models of the human body. Further we redesigned a number of impedance-matched electrodes to allow transmission without stubs or transformers. The specific absorption rate (SAR) and transmission characteristics S_{21} of these electrode structures were compared for several models.

I. INTRODUCTION

Recently, the study of human body communication (HBC) has attracted wide attention as a wireless communication technology for its use in body area networks^[1] (BANs). This technique of using the human body as a signal transmission medium has many advantages. Because signals pass through the human body, they are considerably less susceptible to electromagnetic noise and physical obstacles, as compared with other wireless transmission technologies such as Bluetooth and IrDA. These characteristics suggest several applications for use in health care and elderly support systems as a means of transmitting and collecting bio-sensor information on (and inside) the human body.

In general, a homogeneous model in which all electrical properties are equivalent to that of muscle, was often used for electromagnetic field analysis in HBC. Although actual human tissues are complex in ways that can affect HBC, it is difficult to experiment with the human body in order to evaluate this difference. To overcome these limitations, in this paper, we propose a layered-structure model that consists of concentric layers and use it to perform a mathematical analysis. The remainder of this paper is organized as follows. In section 2, the analysis conditions are described in detail. In section 3, the input impedance characteristics as functions of the electrode structures are calculated using a three-dimensional electromagnetic field simulation. In section 4, we designed several transmitters with an

impedance-matched electrode. Additionally, a comparison among the electric field distribution around the human arm region, the specific absorption ratio (SAR), and the change in the transmission characteristics S_{21} to the receiver electrode attached to a human arm from a transmitter electrode is carried out. In section 5, the conclusions of this paper are presented.

II. OUTLINE OF NUMERICAL ANALYSIS

A. Analysis Model of Human Body

In this study, we examined the communication between wearable devices (transmitters) installed midway down the arm and a mobile terminal (receiver) on the hand. Fig. 1 shows the proposed three-dimensional electromagnetic field analysis model of the human body communication system. This system was analyzed using the finite difference time domain (FDTD) method (Remcom: XFDTD). The human arm was approximated as a circular cylinder of radius r . On the basis of the average arm length of a Japanese adult male^[3], the length of the human arm model in this study was considered to be 700 mm. The surface of the human arm model was flattened at 10 % of the human arm diameter to create a planar surface for contact (the location of plane was 6 mm from the model surface; the width of the plane to which the contact electrodes were attached was $w = 36$ mm).

Fig. 2 shows the cross sections of the arm models. Fig. 2(A) shows a homogeneous model, which has electrical properties equivalent to that of muscle (muscle model) and one that has $2/3$ the dielectric constant and conductivity, taking into consideration the tissues containing water ($2/3$ -muscle model). Fig. 2(B) shows the layered-structure model, which consists of three concentric layers of tissues: skin, fat, and muscle (layered human body model).

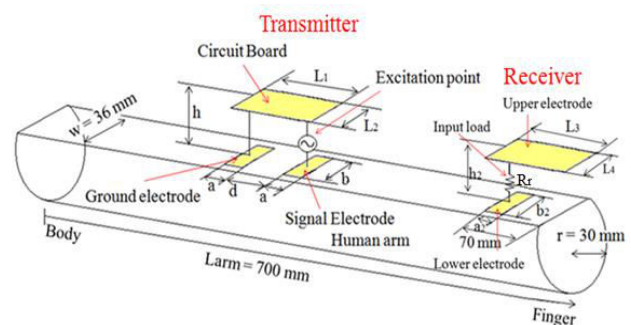


Figure 1. Analysis model of the transmitter and receiver electrode placement on human arm.

Y. Machida is with the Tokyo University of science, 2641 Yamazaki Noda-shi, Chiba, 278-8510 Japan (phone: +81-4-7124-1501; fax: +81-4-7120-1741; e-mail: j7312662@ed.tus.ac.jp).

T. Yamamoto is with the Tokyo University of science, 2641 Yamazaki Noda-shi, Chiba, 278-8510 Japan (e-mail: yamamoto@rs.noda.ac.jp).

K. Koshiji is with the Tokyo University of science, 2641 Yamazaki Noda-shi, Chiba, 278-8510 Japan (e-mail: koshiji@rs.noda.ac.jp).

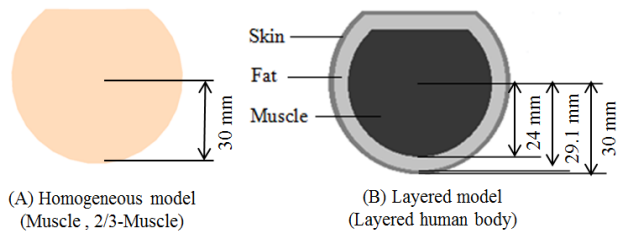


Figure 2. Cross sections of the human arm models

B. Structure of Electrodes for Transmitter

Table 1 lists the basic dimensions of the transmitter electrodes installed midway down the arm. This model is composed of a signal and a ground electrode touching the human body and a circuit board based on the structure used in the preceding thesis^[2]. The parameters of the system are as follows: a is the electrode length, b is the electrode width, d is the distance between the ground electrode and the signal electrode, L_1 is the circuit board length, L_2 is the circuit board width, and h is the distance between the circuit board and the electrodes. An excitation source with an input impedance of 50Ω was connected between the circuit board and the signal electrode using a conductive wire with a diameter of 0.2 mm. The circuit board and the ground electrode were also connected. All of the materials of the transmitter consisted of perfect electric conductors (PECs).

TABLE I. BASIC DIMENSIONS OF THE TRANSMITTER ELECTRODE

a	b	d	h	L_1	L_2
20	30	40	10	80	30

Unit [mm]

C. Optimized Input Impedance

We have determined that the optimum input impedance is 50Ω for the following two reasons. In general, 50Ω is used as the output impedance for large scale integration (LSI) at high frequencies. Therefore, the system cost can be reduced, because existing devices are compatible with this value. Furthermore, if the impedance is optimized at 50Ω by changing the electrode structure, the devices can be downsized without the need for inserting a stub or an impedance conversion circuit.

D. Frequency Analysis

In this study, the analysis model employed a frequency of 10 MHz. The electrical properties of human tissues have shown transmission efficiency peaks at around 10 MHz in our previous studies; thus, we use the industry-science-medical (ISM) band (13.56 MHz). Table 2^[4] summarizes the values used in the analysis of the electrical properties of each kind of human tissue. For the skin properties, we used the average value between the dry and the wet state of the skin because its electrical properties varied with wetness.

TABLE II. VALUES USED IN THE ANALYSIS OF THE LAYERED-STRUCTURE HUMAN ARM MODEL

	σ [S/m]	ϵ_r	Thickness [mm]	ρ [kg/m ³]
Dry skin	0.1973	361.6		
Wet skin	0.366	221.8	0.9	1000
Average skin	0.2816	291.7		
Fat	0.02915	13.76	5.1	850
Muscle	0.6168	170.7	24	1050
2/3 Muscle	0.4112	113.8		1050

E Analysis Method

The cell size in the analysis domain was assumed to be the smallest, i.e., $\Delta x = \Delta y = \Delta z = 1$ mm in the transmitter neighborhood. The cell size gradually increased with an increase in the distance from the domain. The largest cell size was $\Delta x = \Delta y = \Delta z = 5$ mm. The sub-cell method was applied to the arm section to simulate it more exactly, and seven levels of perfect matching layers (PMLs) were applied to the border absorption condition.

III. IMPEDANCE CHARACTERISTICS OF TRANSMITTER ELECTRODE

To determine the transmitter electrode structure required for an input impedance of 50Ω , the input impedance characteristics (Z_{in}) as functions of the electrode structures were calculated using electromagnetic field analysis. When one parameter was varied, the others were fixed at the values listed in Table 1.

Fig. 3 representatively shows the input impedance characteristics as functions of parameters a , b , and d , which have the largest effect. This result indicates that the resistive component and the absolute value of the reactive component of Z_{in} decrease with an increase in the electrode area; further, they increase with a decrease in the electrode distance. The result with a and b is caused by an increase in the current flow into the human body as the electrode area increases. However, it approaches a constant value, even if the electrode area increases, because the current density in the marginal region (where the ground electrode and signal electrode face each other) decreases away from the margin. The result with d depends on the length of the margin region.

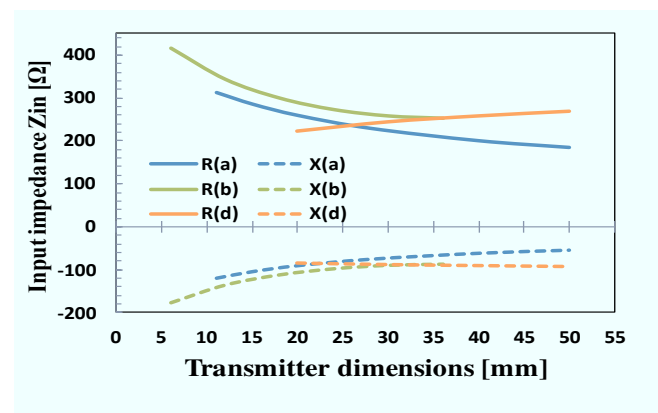


Figure 3. Input impedance characteristics of transmitter electrodes as functions of parameters a , b , and d .

IV. COMPARISON AMONG THE ELECTRIC FIELD DISTRIBUTION, TRANSMISSION CHARACTERISTICS, AND SPECIFIC ABSORPTION RATE IN VARIOUS HUMAN BODY MODELS

In our previous studies, the muscle model and the 2/3-muscle model had similar transmitter electrode input impedance characteristics to those of the layered human body model. In addition, as discussed in section 3, the impedance-matched electrode dimensions can take on a number of combinations by changing the dimensions of the electrodes. The comparison was made in terms of the electric field distribution, transmission characteristics, and specific absorption rate for various human body models for several impedance-matched electrode structures with different dimensions.

The transmission characteristics S_{21} between the transmitter and the receiver were calculated using the electromagnetic field analysis model shown in Fig. 1. On the basis of the dimensions of a mobile phone, the receiver structure of the lower electrode length was $a_2 = 10$ mm, the lower electrode width was $b_2 = 20$ mm, the upper electrode length was $L_3 = 120$ mm, the upper electrode width was $L_4 = 60$ mm, and the distance between the upper electrode and the lower electrode was $h_2 = 10$ mm. The reception resistance $R_r = 2$ k Ω connected the upper electrode to the lower electrode using a conductive wire with a diameter of 0.2 mm. The receiver was placed 260 mm away from the transmitter.

A. Analysis using the Muscle Model

As shown in Table 3 and Fig. 4, we designed an impedance-matched transmitter by selecting the appropriate values of electrode width b and distance between electrodes d , with the electrode length a fixed at 20 mm. By inserting an inductance in series to cancel the reactive component, the values of Z_{in} of (1)(2)(3) were $50.6 - j0.0 \Omega$, $50.5 - j0.0 \Omega$, and $50.8 - j0.0 \Omega$, respectively. The analysis results of the electric field distribution, transmission characteristics S_{21} , and the SAR of (1)(2)(3) are shown in Fig. 5 and Table 4. These results show that as the electrode width b and the distance between the electrodes d decrease, the electromagnetic fields and S_{21} decrease, and the SAR increases.

TABLE III. OPTIMIZED DIMENSIONS OF THE TRANSMITTER ELECTRODES FOR MUSCLE MODEL

	a	b	d	h	L1	L2
(I)	20	28	20	10	60	28
(II)	20	19	10	10	50	19
(III)	20	14	5	10	45	14

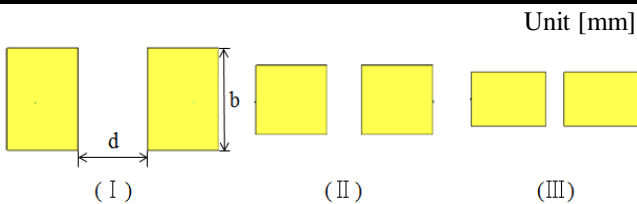


Figure 4. Optimized electrode structure for muscle model.

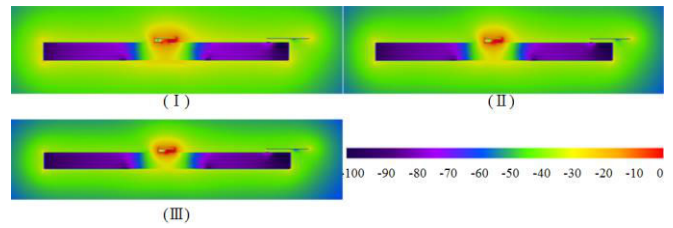


Figure 5. Electric field distribution around and inside the human arm with optimized wearable transmitter for muscle body [dB].

TABLE IV. SAR AND S_{21} CHARACTERISTICS FOR MUSCLE MODEL

	(I)	(II)	(III)
SAR Maximum Value[W/kg]	1.0	1.7	3.0
SAR Average Value per 1 g [W/kg]	0.8×10^{-1}	1.7×10^{-1}	2.8×10^{-1}
SAR Average Value per 10 g[W/kg]	4.0×10^{-2}	6.6×10^{-2}	7.5×10^{-2}
S_{21} [dB]	-46.0	-49.1	-51.3

B. Analysis using the 2/3-Muscle Model

As shown in Table 5 and Fig. 6, we designed the impedance-matched transmitter by selecting the appropriate values of electrode length a and the distance between electrodes d , with the electrode width b fixed at 30 mm. By inserting an inductance in series to cancel the reactive component, the values of Z_{in} of (4)(5)(6) were $50.7 - j0.0 \Omega$, $50.3 - j0.0 \Omega$, and $49.7 - j0.0 \Omega$, respectively. The analysis results of the electric field distribution, transmission characteristics S_{21} , and the SAR of (4)(5)(6) are shown in Fig. 7 and Table 6. These results indicate that as the electrode length a and the distance between the electrodes d decrease, the electromagnetic fields and S_{21} decrease, and SAR increases.

TABLE V. OPTIMIZED DIMENSIONS OF THE TRANSMITTER ELECTRODES FOR 2/3-MUSCLE MODEL

	a	b	d	h	L1	L2
(IV)	54	36	12	10	120	36
(V)	20	36	7	10	47	36
(VI)	6	36	3	10	15	36



Figure 6. Optimized electrode structure for 2/3-muscle model.

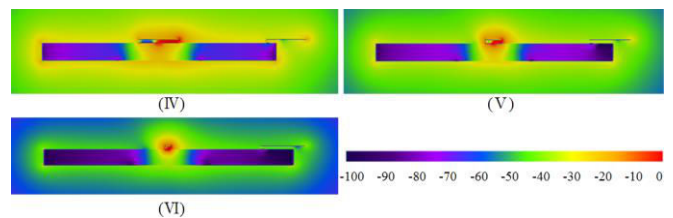


Figure 7. Electric field distribution around and inside the human arm with optimized wearable transmitter for 2/3-muscle [dB].

TABLE VI. SAR AND S_{21} CHARACTERISTICS FOR 2/3-MUSCLE MODEL

	(IV)	(V)	(VI)
SAR Maximum Value[W/kg]	4.4×10^{-1}	8.1×10^{-1}	3.1
SAR Average Value per 1 g [W/kg]	1.0×10^{-1}	1.6×10^{-1}	2.0×10^{-1}
SAR Average Value per 10 g [W/kg]	4.7×10^{-2}	5.6×10^{-2}	5.6×10^{-2}
S_{21} [dB]	-39.6	-47.5	-57.7

C. Analysis using the Layered Human Body Model

As shown in Table 7 and Fig. 8, we designed an impedance-matched transmitter by selecting the appropriate values of electrode length a , electrode width b , and distance between electrodes d . By inserting an inductance in series to cancel the reactive component, the values of Z_{in} of (7)(8)(9) were $49.4 - j0.0 \Omega$, $49.8 - j0.0 \Omega$, and $49.0 - j0.0 \Omega$, respectively. The analysis results of the electric field distribution, transmission characteristics S_{21} , and the SAR of (7)(8)(9) are shown in Fig. 9 and Table 8. From these results, we found that as the electrode length a , electrode width b , and distance between electrodes d decrease, the electromagnetic fields and S_{21} decrease, and the SAR peak increases; however, the average SAR values per 1 g and 10 g of tissue were almost unchanged.

TABLE VII. OPTIMIZED DIMENSIONS OF THE TRANSMITTER ELECTRODES FOR LAYERED HUMAN BODY MODEL

	a	b	d	h	L1	L2
(VII)	30	29	1	10	61	29
(VIII)	15	25	0.8	10	31	25
(IX)	10	18	0.5	10	21	18

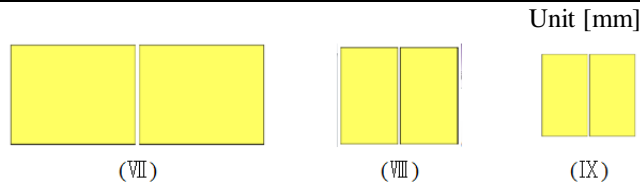


Figure 8. Optimized electrode structure for layered human body model.

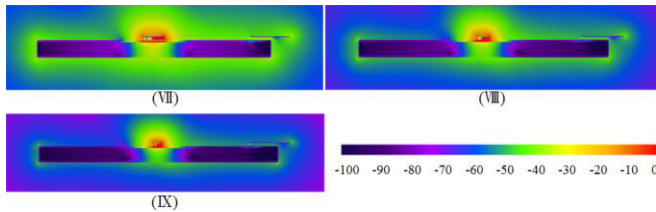


Figure 9. Electric field distribution around and inside the human arm with optimized transmitter for layered human body [dB].

TABLE VIII. SAR AND S_{21} CHARACTERISTICS FOR LAYERED HUMAN BODY

	(VII)	(VIII)	(IX)
SAR Maximum Value[W/kg]	11.7	15.5	27.9
SAR Average Value per 1 g [W/kg]	4.3×10^{-2}	4.6×10^{-2}	4.6×10^{-2}
SAR Average Value per 10 g [W/kg]	1.2×10^{-2}	1.2×10^{-2}	1.2×10^{-2}
S_{21} [dB]	-52.0	-59.9	-64.6

D. Discussion of Results

As shown in sections IV.B, IV.C, and IV.D, both the electric field distribution surrounding and inside the human body and the transmission characteristics S_{21} decrease in all human arm models as the electrode area and the distance between the ground electrode and the signal electrode decrease. This result is attributed to the fact that the current flow into the human body decreases with a decrease in the electrode area. Furthermore, because the closed-circuit characteristic of the transmitter electrodes becomes pronounced as the distance between the ground electrode and the signal electrode decreases, the current traveling through the body is reduced, and thus, the electric field distribution is reduced. Eventually, the transmission characteristics S_{21} decrease, because S_{21} can reach the potential difference caused by the electric field between the upper electrode and both the lower electrode and the arm portion of the receiver.

The SAR increases with a decrease in the distance between the ground electrode and the signal electrode, because the current density on the edges between the ground electrode and the signal electrode increases. In addition, considering the electrical properties and the electric field distribution in the case of the analysis of the 2/3-muscle and layered human body models, we found that the value of the SAR was less than that obtained in the case of the muscle model. However, the maximum value of the SAR was found in the analysis of the layered human body model because the internal electric field of the skin and the fat layer just below the electrode was stronger.

V. CONCLUSIONS

In this study, we examined the specific absorption rate and transmission characteristics S_{21} for transmitters of several different dimensions using electromagnetic field analysis. Our results for the influence caused by the electric field inside the body on the human body were calculated under the same conditions as mentioned above. The values of the SAR per 10 g of arm tissue and per 1 g of arm tissue were satisfied, based on two regional absorption limits for the use of radio waves: (1) below 1.6 W/kg per 1 g of any tissue in the United States [established by the Federal Communications Commission (FCC)] and (2) below 2 W/kg per 10 g of any tissue in Japan [established by International Commission on Non-Ionizing Radiation Protection (ICNIRP)]. The transmission characteristics S_{21} were also influenced not only by the human arm model being analyzed but also by the properties of the transmission devices, particularly the parameters of the electrode area and the distance.

REFERENCES

- [1] T. G. Zimmerman : "Personal Area Networks (PAM) : Near-Field Intra-Body Communication", M. S. thesis, MIT Media Laboratory,(1995)
- [2] K. Hachisuka, T. Takeda, Y. Terauchi, K. Sasaki, H. Hosaka and K. Itao : "Intra-Body Data transmission for the Personal area Network", *Microsystem Technologies*, Vol. 11, No.8-10, pp. 1020-1027, 2005
- [3] "Human body dimensions data for ergonomic design", ISBN4-88922-093-3 C3040 P4635E, 1996.6.
- [4] Dielectric Properties of Body Tissues in the frequency range 10Hz-100GHz <http://niremf.ifac.cnr.it/tissprop/>